

Supplemental Information

ATP Alters the Diffusion Mechanics

of MutS on Mismatched DNA

Won-Ki Cho, Cherlhyun Jeong, Daehyung Kim, Minhyeok Chang, Kyung-Mi Song, Jeunghill Hanne, Changill Ban, Richard Fishel, and Jong-Bong Lee

Inventory of Supplemental Information

Figure S1: Schematic representation of the 15.3 kb DNA and colocalization of 15.3kb DNA and Alexa647 attached to the DNA. Related to Figure 1.

Figure S2: The net displacement of MutS and diffusion coefficient of ATP-bound MutS in the absence of the hydrodynamic force. Related to Figure 2.

Movie S1: Video clips showing the movement of ATP-bound MutS sliding clamps at the flow rate of 0.15 ml/min (top) and 0.75 ml/min (bottom). Related to Figure 2.

Movie S2: Video clips showing multiple ATP-bound MutS sliding clamps diffusing along 15.3 kb mismatched DNA. Related to Figure 3.

Figure S3: Filtering of undesired and abnormal trajectories. Related to Figure 3.

Table S1: DNA substrates for the polarization analysis. Related to Figure 4 and 5.

Figure S4: The analyses of polarization. Related to Figure 4.

Supplemental Methods:

- Constructing a 15.3 kb DNA containing a single mismatch.
- Calculation of the diffusion coefficient.

Supplemental Data

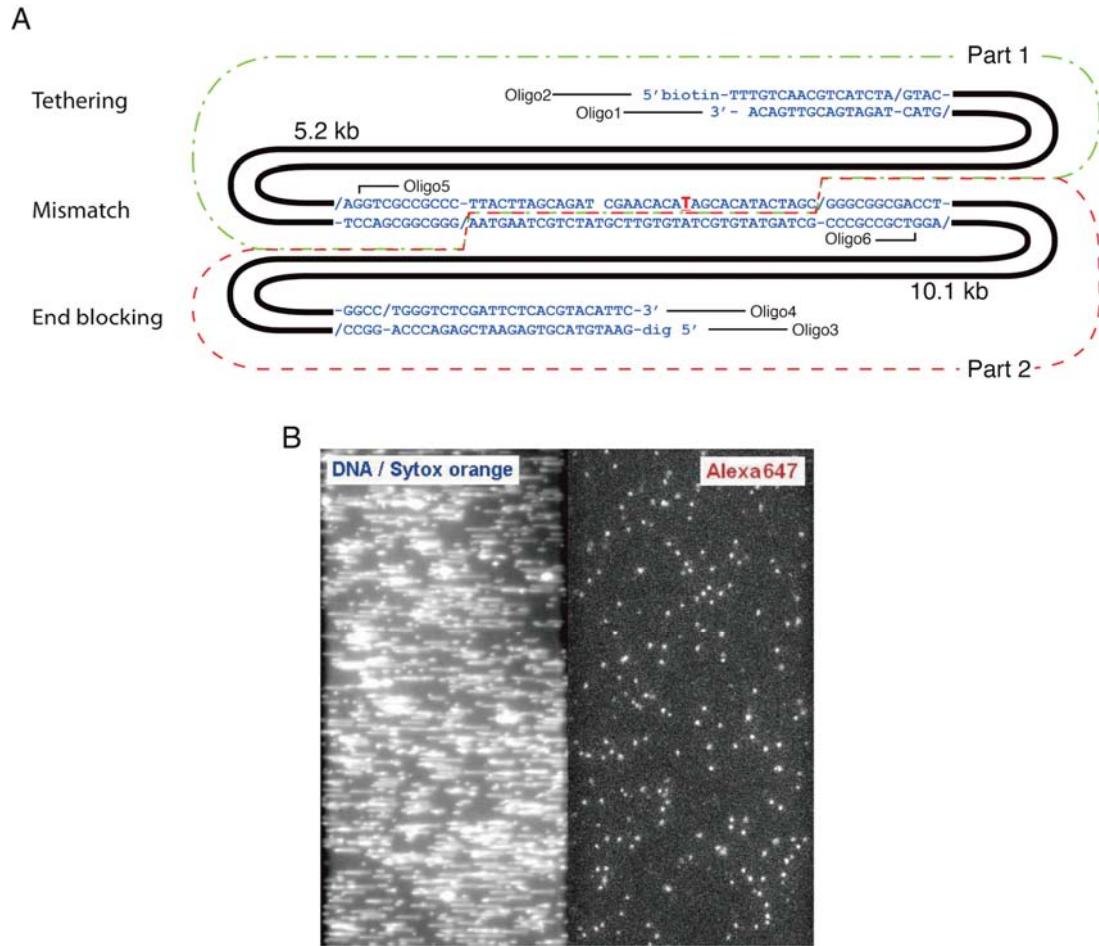


Figure S1, related to Figure 1: Schematic Representation of the 15.3 kb DNA and colocalization of 15.3 kb DNA and Alexa647 Attached to the DNA. (A) Construct of a 15.3 kb DNA containing a single mismatch (see also Supplemental Methods). **(B)** The flow-stretched 15.3 kb DNA molecules were imaged simultaneously to visualize the intercalator Sytox Orange that distributes non-specifically along the entire DNA length and Alexa647 fluorophore that is located 9 bp from the mismatch. We find that 85% of the DNA molecules contain the Alexa647 label.

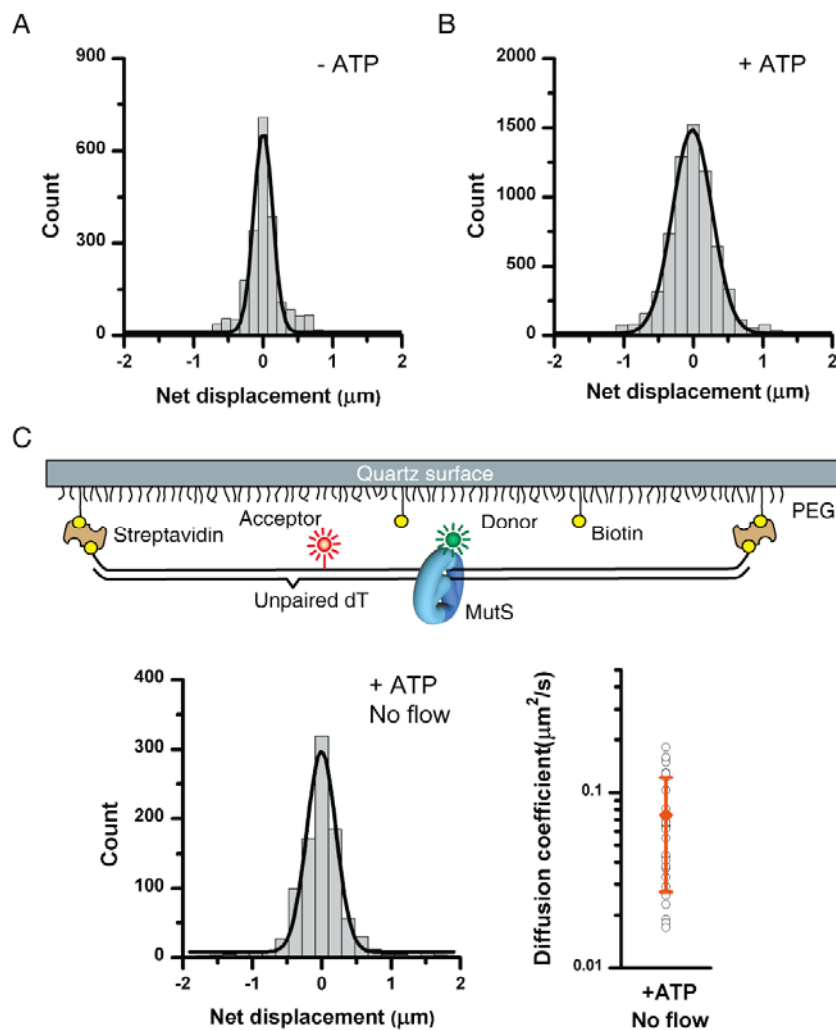


Figure S2, related to Figure 2: The Displacement of MutS Positions Between Two Sequential EMCCD Camera Frames and Diffusion Coefficient of ATP-bound MutS in the Absence of the Hydrodynamic Force. (A) Histogram of the net displacement of MutS searching a mismatch in the absence of ATP. The mean of the displacement is 2 nm (\pm 6 nm) (62 trajectories). **(B)** The mean displacement of ATP-bound MutS is -14 nm (\pm 5 nm) (54 trajectories). These studies were performed in 50 mM NaCl and 200 μ M ATP when present. The small deviation from zero indicates that the hydrodynamic force used to stretch the immobilized DNA does not bias the MutS motion on the DNA at the flow rate of 0.15 ml/min. Displacement measured at other ionic strength was not significantly different. **(C)** Biotin-labeled on both ends of 15.3 kb DNA were tethered on the flow-cell surface via biotin-streptavidin interaction under the flow rate of 0.50 ml/min. The resulting extended and doubly tethered DNA allowed us to follow individual MutS proteins diffusing on the DNA in the absence of the stretching hydrodynamic force. The mean displacement of ATP-bound MutS

with no flow is -4 nm ($\pm 10 \text{ nm}$; 31 trajectories) in the presence of 100 mM NaCl and 1 mM ATP (see the left histogram). The distribution of the diffusion coefficient of the ATP-bound MutS clamps shows $0.075 \pm 0.047 \text{ } \mu\text{m}^2/\text{s}$ (mean \pm s.d.; see the right distribution), which is nearly identical to that in the presence of flow at 100 mM NaCl ($0.087 \text{ } \mu\text{m}^2/\text{s}$ in average; Figure 2B). These results suggest that the flow used to stretch the DNA does not affect the diffusion of both a searching and ATP-bound *Taq*MutS.

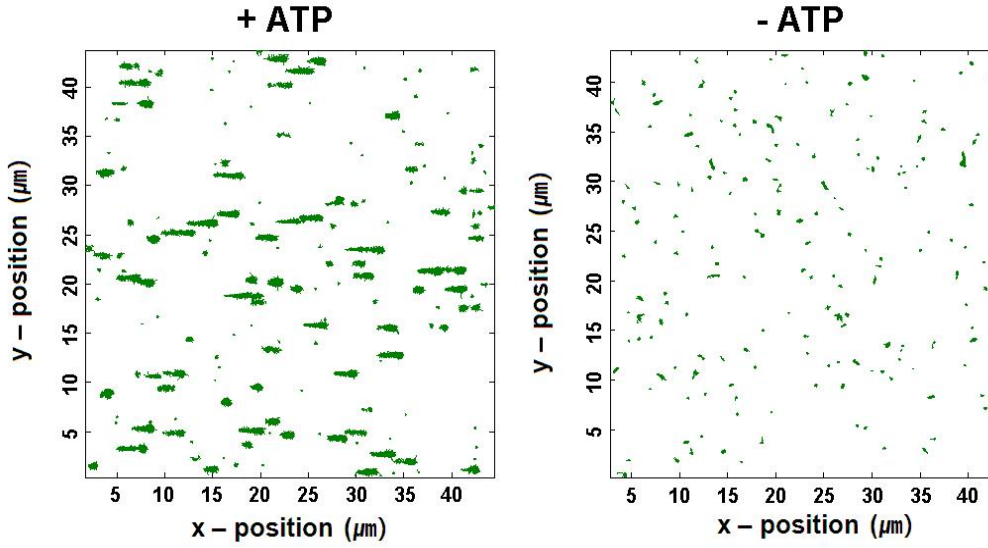


Figure S3, related to Figure 3: Filtering of Undesired and Abnormal Trajectories. We filter these abnormal trajectories using the asymmetry test (Huet et al., 2006; Jaqaman et al., 2008). The asymmetry S of a trajectory is given by:

$$S = -\ln \left(1 - \frac{(\lambda_1 - \lambda_2)^2}{(\lambda_1 + \lambda_2)^2} \right)$$

where λ_1 and λ_2 are the eigenvalues of the variance-covariance matrix of the particle positions along the trajectory. When MutS moves on the stretched DNA along the x-axis, λ_1 and λ_2 corresponds to σ_1^2 and σ_2^2 , respectively. σ_1 and σ_2 is the standard deviation of the mean position along x-direction and y-direction, respectively. For ATP-bound MutS, its trajectory length is at least 20 frames (1 s) and $S > 1$. As a result, the standard deviation of the mean position along the x-direction is 3 fold greater than that along the y-direction (asymmetry test). We also ignore the trajectories if the angle between the slope of the MutS positions in a trajectory and the flow direction is greater than $\pi/18$ (1D directional test). The threshold angle was determined from the fluctuation of DNA at 0.15 ml/min and represents the maximum trajectory deviation of particles that are clearly moving along the DNA.

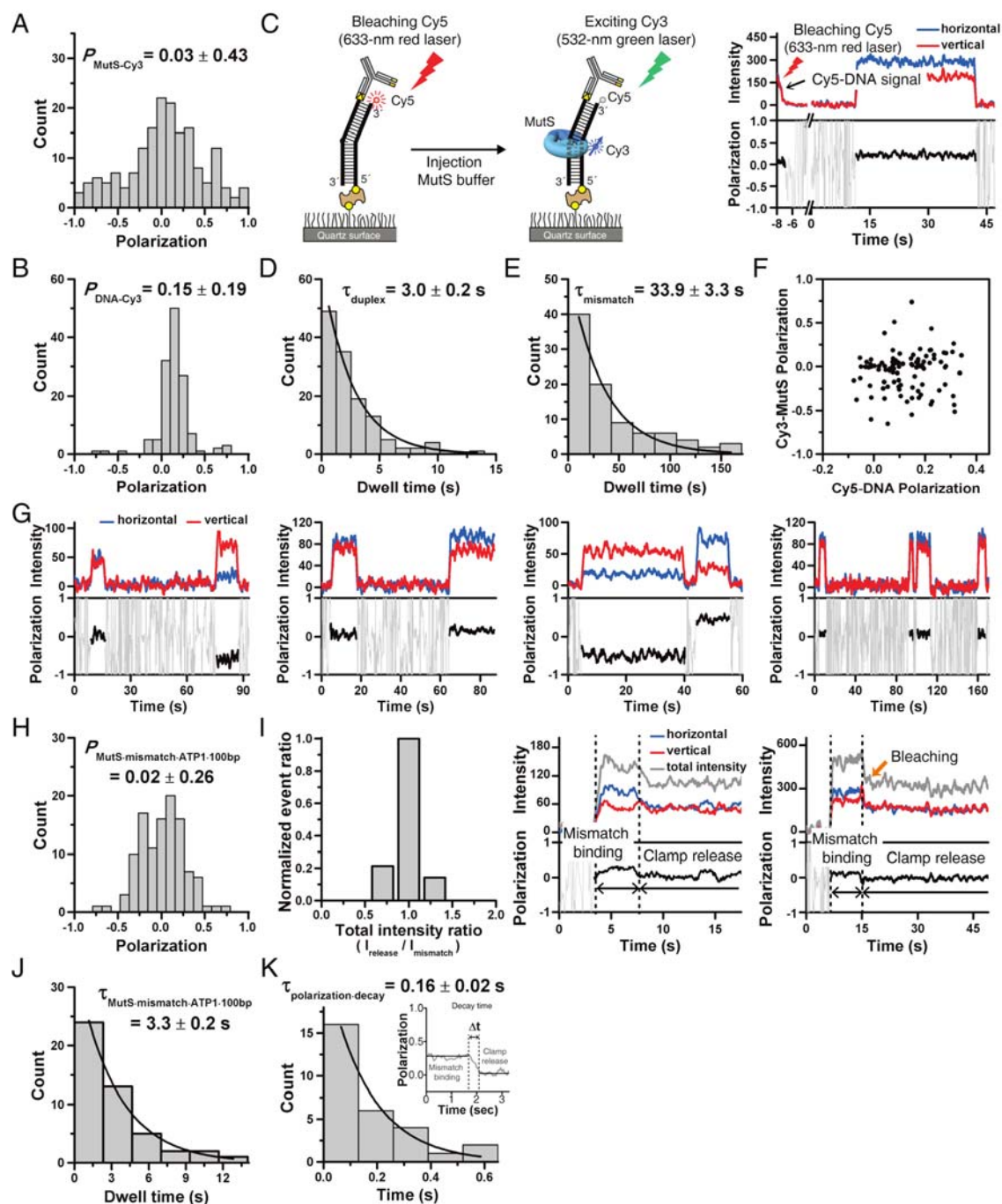


Figure S4, related to Figure 4: The Analyses of Polarization. (A) The steady-state polarization of Cy3-MutS nonspecifically immobilized on the surface, which results in the random distribution of the MutS on the surface. The resulting Cy3-MutS polarization is broadly distributed from -1.0 to 1.0 . These results indicate that a rigid linkage to the MutS protein suppresses the rotational freedom of the Cy3. **(B)** The steady-state polarization of Cy3 attached to a DNA substrate that is immobilized on the surface via a streptavidin-biotin

linker. The non-zero polarization and moderately wide distribution of $P_{\text{Cy3-DNA}}$ suggests that the DNA orientation is ordered. These results are consistent with Cy3 stacking onto the base pair of the DNA end (Iqbal et al., 2008). Such an anisotropy of the Cy3-MutS and Cy3-DNA enables the measure of rotational dynamics within our 50 ms sampling time. **(C)** MutS may bind nonspecifically to the flow-cell surface. To assure we are examining MutS bound to a mismatch we first localize the Cy5-DNA. To eliminate any FRET, the Cy5 fluorophore is completely photobleached with the 633 nm laser (left). The Cy3-MutS is then injected into the flow cell (middle) and the Polarization recorded (right). Representative polarization data collected from a trace that initially shows a Cy5 signal. **(D)** Histogram of the dwell time of MutS on 100 bp duplex DNA. **(E)** Histogram of the dwell time of MutS on the 100 bp unpaired dT mismatched DNA. The dwell times (3.0 s, 33.9 s) measured from polarization traces in the presence of 100 mM NaCl were nearly identical (3.7 s, 36.5 s) to those previously measured by smFRET (Jeong et al., 2011). **(F)** No correlation between the polarization of Cy3-MutS and Cy5-DNA where the fluorophore is presumably stacked onto the end base pair. These results suggest that the orientation of mismatch-bound MutS is independent of the orientation of DNA. The Pearson's correlation coefficient is 0.07. **(G)** These observations suggest that there are a variety of polarizations of different MutS proteins bound to the mismatch on the same 100 bp DNA template. **(H)** The distribution of polarization was determined for the initial mismatch binding state in the presence of ATP (1 mM). The distribution is identical to that in the absence of ATP (Figure 4C). **(I)** The distribution of the total intensity rate (20 trajectories). Approximately 70% of the events show no significant change of the total intensity within the signal to noise ratio of the system (left). A representative trace where the total intensity decreases due to the decrease of I_H , but no change of I_V (middle). A representative trace where both intensities decrease (right). This latter observation may be due to photobleaching of one of two Cy3 dyes that are conjugated to a single MutS (a condition that may happen with 10% of the Cy3-MutS). **(J)** The dwell time from polarization traces in the presence of 100 bp unpaired dT mismatched DNA in 100 mM NaCl, and 1 mM ATP is identical to that previously measured by the smFRET system in the presence of 100 mM KCl (Jeong et al., 2011). **(K)** In the presence of ATP, a time trace shows two distinct polarization states: the initial mismatch binding state and the second ATP-bound MutS state. We examined the decay time (Δt) from the mismatch binding state to the ATP-bound MutS state (Inset). The decay times in the single-molecule traces were determined as follows: the polarization data of the two states were averaged and fitted with line segments parallel to x-axis. The two points at which the slope-fitted line segment crosses the two line segments of the two polarization states were chosen for the decay time (Inset). The mean decay time is 0.16 s.

Table S1, related to Figure 4 and 5: DNA Substrates for the Polarization Analysis.

DNA duplex		Strand sequence (5' to 3')	Modification
100 bp matched DNA	100 nt	GTTACCGATACGATACGAATAGGCATATCTGCACG TTTCTCACGAGGCGCCGCTAGAC <u>I</u> GATCTGGAGCT TAATTGCCTGCCGGAGCTAAAGACGTTCCA	5': Biotin <u>I</u> : amino-dT+Cy5
	100 nt	TGGAACGTCTTTAGCTCCGGCAGGCAATTAAGCTC CAGATCAGTCTAGCGGCGCCTCGTGAGAAACGTG CAGATATGCCTATTCGTATCGTATCGGTAAC	5' : Biotin
100 bp mismatched DNA	100 nt	GTTACCGATACGATACGAATAGGCATATCTGCACG TTTCTCACGAGGCGCCGCTAGAC <u>I</u> GATCTGGAGCT TAATTGCCTGCCGGAGCTAAAGACGTTCCA	5': Biotin <u>I</u> : amino-dT+Cy5
	101 nt	TGGAACGTCTTTAGCTCCGGCAGGCAATTAAGCTC CAGATCAGTCTAGCGTGCCTCGTGAGAAACGT GCAGATATGCCTATTCGTATCGTATCGGTAAC	5' : Biotin
74 bp matched DNA	74 nt	ATTCAGCTGTACCCAATTCACTCTACGACGAGGCG TCGCTAGCG <u>I</u> CGCATCCTGCTGTAAGTTTCATGTC CACC	5': Biotin <u>I</u> : amino-dT+Cy5
	74 nt	GGTGGACATGAACTTACAGCAGGATGCGACGCT AGCGACGCCTCGTCGTAGAGTGAATTGGGTACAG CTGAAT	5' : digoxigenin
74 bp mismatched DNA	74 nt	ATTCAGCTGTACCCAATTCACTCTACGACGAGGCG TCGCTAGCG <u>I</u> CGCATCCTGCTGTAAGTTTCATGTC CACC	5': Biotin <u>I</u> : amino-dT+Cy5
	75 nt	GGTGGACATGAACTTACAGCAGGATGCGACGCT AGCGTACGCCTCGTCGTAGAGTGAATTGGGTACA GCTGAAT	5' : digoxigenin
45 bp matched DNA	45 nt	TCTGCACGTTTCTCACGAGGCGCCGCTAGAC <u>I</u> GAT CTGGAGCTTA	5': Biotin <u>I</u> : amino-dT+Cy5
	45 nt	TAAGCTCCAGATCAGTCTAGCGGCGCCTCGTGAG AAACGTGCAGA	5' : Biotin
45 bp mismatched DNA	45 nt	TCTGCACGTTTCTCACGAGGCGCCGCTAGAC <u>I</u> GAT CTGGAGCTTA	5': Biotin <u>I</u> : amino-dT+Cy5
	46 nt	TAAGCTCCAGATCAGTCTAGCGTGCCTCGTGA GAAACGTGCAGA	5' : digoxigenin
30 bp matched DNA	30 nt	CAGATCAGTCTAGCGGCGCCTCGTGAGAAC	5': Biotin 3': Cy5
	32 nt	TTGTTCTCACGAGGCGCCGCTAGACTGATCTG	5' : digoxigenin
30 bp mismatched DNA	30 nt	CAGATCAGTCTAGCGGCGCCTCGTGAGAAC	5': Biotin 3': Cy5
	33 nt	TTGTTCTCACGAGGCGCTCGCTAGACTGATCTG	5' : digoxigenin
26 bp matched DNA	26 nt	GATCAGTCTAGCGGCGCCTCGTGAGA	5': Biotin 3': Cy5
	28 nt	TTTCTCACGAGGCGCCGCTAGACTGATC	5' : digoxigenin
26 bp mismatched DNA	26 nt	GATCAGTCTAGCGGCGCCTCGTGAGA	5': Biotin 3': Cy5
	29 nt	TTTCTCACGAGGCGCTCGCTAGACTGATC	5' : digoxigenin

Supplemental Methods

Constructing a 15.3 kb DNA containing a single mismatch.

We constructed 15.3 kb DNA containing an unpaired dT and an Alexa647 fluorophore that does not interfere with MutS binding and may be used as a FRET acceptor from a Cy3 donor. The final DNA is composed of three constituent elements (blue-colored sequences in Figure S1A): Tethering, Mismatch, and End blocking (see left labels in Figure S1A). The Tethering and half of the Mismatch elements were coupled with ends of a 5.2 kb DNA (Figure S1A, Part 1). The other half of the Mismatch and End blocking elements were linked to ends of a 10.1 kb DNA (Figure S1A, Part 2). We followed the manufacturers protocols for restriction, phosphorylation, and ligation. All oligos were purchased from IDT (blue-colored sequences in Figure S1A).

Alexa647 (Monofunctional NHS-ester, Invitrogen) was covalently conjugated to the amine-modified dT base (**T** in the above figure) on Oligo5 via six carbon linkers. The labeling efficiency was 85%. The labeling procedures have been described previously (Jeong et al., 2011). λ DNA was digested with BsrGI or ApaI, which results in 5,204 bp (5.2 kb) and 10,076 bp (10.1 kb) fragments that contain a 4 nt single stranded DNA (ssDNA) 5'-overhang and the 12 nt ssDNA left cohesive end (*cosL*) of λ , respectively. The fragments were isolated from a 0.5% agarose gel and were eluted by QIAquick Gel Extraction Kit (QIAGEN). The Alexa647-labeled and purified Oligo5 as well as Oligo6 were phosphorylated with T4 Polynucleotide Kinase (Roche). Oligo1 and Oligo4 were not phosphorylated to prevent self-ligation of the Tethering and End blocking elements.

For Part 1, the *cosL* tail of the 5.2 kb fragment was annealed and ligated with the 47 nt ssDNA Alexa647-Oligo 5 (Figure S1A), and the BsrGI tail of the 5.2 kb fragment was annealed and ligated with the 21 nt 5'-biotin ssDNA (Oligo 2) and 19 nt complementary ssDNA linker (Oligo 1) using T4 DNA ligase (Roche) at room temperature overnight. For Part 2, the *cosL* tail of 10.1 Kb fragment was annealed and ligated with a 48 nt ssDNA containing an unpaired dT (Oligo 6), and the ApaI tail of the 10.1 kb fragment was annealed and ligated with the 29 bp 5'-digoxigenin dsDNA (Oligo 3 and 4) using T4 DNA ligase (Roche) at room temperature overnight.

The Part 1 and Part 2 fragments were isolated from a 0.5% agarose gel and eluted by QIAquick Gel Extraction Kit (QIAGEN), annealed by heating to 70 °C and slow cooling to room temperature, followed by ligation with T4 ligase (Roche) at room temperature overnight. The resulting 15.3 kb DNA was isolated from a 0.5% agarose gel and eluted by a QIAEX II Gel Extraction Kit (QIAGEN) and stored at 4 °C.

Calculation of the diffusion coefficient (*D*).

The position of MutS was determined by Gaussian fitting of the intensity profile of Cy3-labeled MutS using DiaTrack 3.0 (Semasopt) (Lee et al., 2006). The diffusion coefficient (*D*) for Cy3-labeled MutS diffusing on 15.3 kb DNA molecule was determined from the slope of a mean-square displacement (MSD) versus time using the equation $MSD(t) = 2Dt$ where *t* is the time interval. 10% of the total measurement time was taken for the fitting points (Gorman et al., 2007; Qian et al., 1991). The mean-square displacement (*MSD*) of each MutS molecules was calculated by:

$$MSD(t) = \frac{1}{N} \sum_{i=1}^N (x_i(t) - x_i(0))^2$$

where $t = n\Delta T$ ($n=1, 2, 3, \dots, \Delta T$: sampling rate).

References

- Gorman, J., Chowdhury, A., Surtees, J.A., Shimada, J., Reichman, D.R., Alani, E., and Greene, E.C. (2007). Dynamic basis for one-dimensional DNA scanning by the mismatch repair complex Msh2-Msh6. *Mol Cell* 28, 359-370.
- Huet, S., Karatekin, E., Tran, V.S., Fanget, I., Cribier, S., and Henry, J.P. (2006). Analysis of transient behavior in complex trajectories: application to secretory vesicle dynamics. *Biophys J* 91, 3542-3559.
- Iqbal, A., Arslan, S., Okumus, B., Wilson, T.J., Giraud, G., Norman, D.G., Ha, T., and Lilley, D.M. (2008). Orientation dependence in fluorescent energy transfer between Cy3 and Cy5 terminally attached to double-stranded nucleic acids. *Proc Natl Acad Sci U S A* 105, 11176-11181.
- Jaqaman, K., Loerke, D., Mettlen, M., Kuwata, H., Grinstein, S., Schmid, S.L., and Danuser, G. (2008). Robust single-particle tracking in live-cell time-lapse sequences. *Nat Methods* 5, 695-702.
- Jeong, C., Cho, W.K., Song, K.M., Cook, C., Yoon, T.Y., Ban, C., Fishel, R., and Lee, J.B. (2011). MutS switches between two fundamentally distinct clamps during mismatch repair. *Nat Struct Mol Biol* 18, 379-385.
- Lee, J.B., Hite, R.K., Hamdan, S.M., Xie, X.S., Richardson, C.C., and van Oijen, A.M. (2006). DNA primase acts as a molecular brake in DNA replication. *Nature* 439, 621-624.
- Qian, H., Sheetz, M.P., and Elson, E.L. (1991). Single particle tracking. Analysis of diffusion and flow in two-dimensional systems. *Biophys J* 60, 910-921.